Double Mutant Cycle Thermodynamic Analysis of the Hydrophobic Cdc42−ACK Protein−Protein Interaction†

Andrea E. Elliot-Smith, Darerca Owen,* Helen R. Mott, and Peter N. Lowe

Department of Biochemistry, University of Cambridge, 80 Tennis Court Road, Cambridge CB2 1GA, U.K.

Received August 2, 2007; Revised Manuscript Received October 1, 2007

ABSTRACT: Protein−protein interactions such as those between small G proteins and their effector proteins control most cell signaling pathways and thereby govern many cellular processes in both normal and disease states. Each small G protein interacts with several effectors, some shared between similar G proteins and others unique to a single GTPase. Although there is knowledge of the structural basis of these interactions, there is limited understanding of their thermodynamic basis. This is particularly significant because of the intrinsic conformational flexibility of the interacting partners. Here we have conducted a double mutant thermodynamic cycle for two key hydrophobic interactions in the Cdc42−ACK interface: $Val42^{Cdc42}$−$Ile463^{ACK}$ and $Leu174^{Cdc42}$−$Leu449^{ACK}$. Val42 and Leu174 are known to be energetically important in this complex from previous thermodynamic studies, and their respective partners were predicted from the structure of the complex. Such a study has not been hitherto performed on any hydrophobic protein−protein interaction. The results confirm that a significant proportion of the overall interaction is dependent upon these residues, but in neither case is the direct interaction between the side chains the predominant energetic force. Indeed, the interaction of the side chains of Val42 and Ile463 appears to exert an energetic penalty. Rather, the stabilization of the complex, which requires the presence of these two pairs of residues, appears to be due to conformational changes, or interactions, that are not easily visualized in the structure of the complexes. In this respect, it is noteworthy that isolated Cdc42 shows regions of disorder and isolated ACK has no stable tertiary structure, whereas the Cdc42−ACK complex has a well-defined quaternary structure. Such changes may well be critical for the known selectivity of Cdc42 and related proteins such as Rho and Rac, for their wide range of effectors.

Members of the Rho family of small GTP[1] binding proteins, including Rho, Rac, and Cdc42, play important roles in the control of cell growth, differentiation, and migration (*1*). They act as molecular switches, interconverting between GDP-bound (inactive) and GTP-bound (active) forms. In response to stimuli, G proteins are activated to their GTP-bound form, in which state they are conformationally competent to interact with a large variety of downstream effector proteins (*2*). Several targets of the Rho family proteins have been identified, as have multiple regulatory proteins. Biochemical and structural characterization of these interactions has improved our understanding of these functional relationships (*3*).

An important question in small G protein biology is how these GTPases recognize and bind their effector proteins and which residues contribute to this specificity, particularly given the high degree of sequence similarity between Rho family proteins. For example, Cdc42 and Rac are 72% identical, and while some effectors such as the serine/threonine kinase PAK (p21-activated kinase) are common to both, others interact specifically with only one of these GTPases. One effector that specifically interacts with Cdc42 but not Rac is ACK, a tyrosine kinase (*4*) implicated in integrin signaling (*5*) and clathrin-mediated endocytosis (*6*). Extensive mutagenesis studies on the interaction between Cdc42 and ACK (as well as two other CRIB effector proteins) have identified energetically key residues for these interactions (*7*, *8*). The analysis of single-residue mutations generally, however, enables only the relative energies of having one residue versus another (usually alanine) at a specific position to be determined. It is therefore difficult to identify how much the loss of a specific interaction contributes to the effect of a mutation in comparison with other effects on the protein (e.g., structural changes). Double mutant cycle analysis is an analytical technique that can, however, determine the interaction energy between two specific residues, eliminating any effects that may result from changes in solvation or reorganization energies as a result of the mutation (*9*).

Double mutant cycle analysis was first used to analyze enzyme−substrate interactions in tyrosyl-tRNA synthetase (*10*). Since then, it has been used extensively in the study of protein folding mechanisms (in particular of barnase) (*11*−

† This research was supported by a BBSRC Studentship to A.E.E.-S. and CR-UK project Grants C1465/A2590 and C11309/A5148.

* To whom correspondence should be addressed. Telephone: +44-1223-764824. Fax: +44-1223-766002. E-mail: do@bioc.cam.ac.uk.

[1] Abbreviations: CRIB, Cdc42−Rac interactive binding; GDP, guanosine 5′-diphosphate; GTP, guanosine 5′-triphosphate; PAK, p21 activated kinase; ACK, activated Cdc42-associated kinase; WASP, Wiskott-Aldrich syndrome protein; GST, glutathione *S*-transferase; IPTG, isopropyl β-D-thiogalactopyranoside; PEP, phosphoenolpyruvate; DTT, dithiothreitol; SPA, scintillation proximity assay; ITC, isothermal titration calorimetry; GMPPNP, guanylyl 5′-imidodiphosphate; wt, wild type.

10.1021/bi701539x CCC: $37.00
Published on Web 11/14/2007

15), protein−protein interactions (*16*−*19*), antibody−antigen interfaces (*20*), protein−DNA interactions (*21*), and even intermolecular interactions of fluorinated aromatic rings (*22*).

However, the majority of these studies have involved the interaction of hydrophilic residues in folding and binding. Hydrophobic interactions (as analyzed in this work) have not been studied as extensively by double mutant cycle analysis, and those that have been studied involved investigation of the burial of hydrophobic residues during protein folding (*14*) or have replaced hydrophobic residues with charged residues (*19*). Hydrophobic interactions in protein−protein binding have not been studied by mutation to alanine using this method. Alanine is the substituted amino acid of choice as it lacks a side chain beyond the β-carbon and, unlike glycine, does not exhibit unusual backbone dihedral angles (*23*). Thus, the study of the hydrophobic Cdc42−ACK interface through double mutant analysis is of interest to the investigation of protein−protein interactions in general.

Our previous work identified two mutations in Cdc42 that specifically abrogated a particular effector interaction (at least within the CRIB family of effectors) and also contributed significantly to the binding energy (*7*). The total binding energy of the interaction between Cdc42 and ACK has been previously calculated to be 10.15 kcal/mol (*7*). Of this, Val42 contributes 1.54 kcal/mol and Leu174 contributes 1.86 kcal/mol. Mutations of both residues to alanine disrupted ACK binding while not affecting binding to PAK. The L174A mutation, but not V42A, also affects binding to the Wiskott-Aldrich syndrome protein (WASP). From the structure of the Cdc42−ACK complex (*24*), Val42 of Cdc42 packs against Ile463 of ACK while Leu174 contacts Leu449 of ACK. The properties of these mutants indicate that they are potentially useful in the dissection of effector signaling pathways. In addition, their selectivity, coupled with their thermodynamic contribution to complex formation, suggests that they could be potential "hot spots" for targeting small molecule therapies to inhibit interaction with specific effectors. The studies described here aim to confirm whether the loss of an interaction with a single specific effector residue (as indicated by the structure) could explain the change in affinity for ACK when Val42 and Leu174 are mutated in Cdc42 or whether other factors such as loss of multiple interactions or conformational changes contribute.

MATERIALS AND METHODS

Expression Constructs and Recombinant Protein Production

All proteins were expressed as glutathione *S*-transferase fusions in the pGEX series of expression vectors (GE Healthcare). Constructs expressing PAK_{75-118} (*25*) and $ACK_{448-489}$ (*24*) were kind gifts. Cdc42 Δ7 Q61L and mutants were expressed in pGEX 2T from constructs cloned into the *Bam*HI and *Eco*RI sites (*7*, *26*).

Site-directed mutagenesis of the $ACK_{448-489}$ expression construct was performed using the QuikChange or QuikChange multi Site-Directed Mutagenesis Kit (Stratagene). The mutations were confirmed by sequence analysis on an automated sequencer (Applied Biosystems Inc.) by the Department of Biochemistry DNA Sequencing Facility, University of Cambridge.

GST fusion proteins were expressed in *Escherichia coli* XL1-Blue cells (Stratagene) or BL21 (Novagen Inc.), purified, thrombin-cleaved as appropriate, and quantified, as previously described (*8*).

Bound nucleotides were replaced with [^{3}H]GTP by nucleotide exchange in the presence of a GTP regeneration system as previously described (*8*). Bound nucleotides were replaced with GTP in the same way, except that the reaction mixture consisted of 50 mg of Cdc42 Δ7 Q61L, 7 mM GTP, 15 mM phosphoenolpyruvate (PEP), 15 mM KCl, 0.36 M ammonium sulfate, and 120 units of pyruvate kinase.

Scintillation Proximity Assays (SPAs)

Direct Binding SPAs. In the direct binding SPAs, the GST effector proteins, at constant concentrations of 0.05 and 0.08 μM for GST−PAK and GST−ACK fusion proteins, respectively, were immobilized on Protein A SPA fluoromicrospheres (GE Healthcare) via an anti-GST antibody (Molecular Probes, Invitrogen). The equilibrium dissociation constants (K_d) of the effector−G protein interaction were determined by monitoring the SPA signal in the presence of varying [^{3}H]GTP•Cdc42 concentrations as described previously (*25*, *27*). The highest sample concentrations of [^{3}H]GTP•Cdc42 used were 1 and 1.5 μM with GST−PAK and GST−ACK, respectively. In each case, a blank experiment was performed in the absence of GST effector, where increasing the concentration of [^{3}H]GTP•Cdc42 resulted in a linear increase in background SPA counts. The background counts were subtracted from the data points obtained in the presence of the GST effector and the resulting values plotted as a function of increasing Cdc42 concentration. For each affinity determination, data points were obtained for at least 10 different G protein concentrations.

Binding curves were fitted using the appropriate binding isotherms (*25*, *27*) to yield K_d values and their standard errors for the G protein−effector interactions.

Competition SPAs. In the competition assays, thrombin-cleaved and -purified ACK or ACK mutant fragment was titrated into a mixture of 0.035 μM [^{3}H]GTP•Cdc42 and 0.05 μM GST−PAK_{75-118} or 0.03 μM GST−$ACK_{448-489}$ immobilized on fluoromicrospheres as described above. The ACK fragment competes with the GST effector for binding to [^{3}H]GTP•Cdc42 and, therefore, abolishes the scintillation signal. The highest sample concentrations of free ACK peptide that were used were 2 μM. In each case, a blank was performed in the absence of GST effector.

Free GST distorts the SPA results by tightly binding to anti-GST and thus competing with GST−ACK for binding to the SPA beads. As it was possible that small amounts of GST contaminated the cleaved ACK preparation, control experiments were performed, where [^{3}H]GTP•Cdc42 was prebound to SPA beads and cleaved ACK fragments were titrated in. The levels of contaminating GST could then be estimated by the reduction in the magnitude of the scintillation signal. The competition experiments were performed at ACK concentrations where there was no significant loss of signal in these controls.

For each G protein−effector affinity determination, data points were obtained for at least 10 different ACK fragment concentrations. K_d values and their standard errors were obtained by fitting the dose−response curves to binding

isotherms, which describe competition between two proteins binding to one site on another protein, and account for mutual depletion of the interacting components. The value of K_d for the GST effector−Cdc42 interaction was also required, and this was obtained from direct binding SPAs. The equations used were adapted for SPAs from the previously published derivations (*28*, *29*) as follows.

For a system where component A is in the presence of two ligands (B and C), which compete for a single binding site on A and the total concentrations of A, B, and C are $[A]_0$, $[B]_0$, and $[C]_0$, respectively:

$$AB \overset{K_{dAB}}{\rightleftharpoons} A + B$$

$$AC \overset{K_{dAC}}{\rightleftharpoons} A + C$$

$$K_{dAB} = \frac{[A][B]}{[AB]} \quad (1)$$

$$K_{dAC} = \frac{[A][C]}{[AC]} \quad (2)$$

$$[B]_0 = [B] + [AB] \quad (3)$$

$$[C]_0 = [C] + [AC] \quad (4)$$

$$[A]_0 = [A] + [AB] + [AC] \quad (5)$$

Rearranging [B] and [C] in eqs 3 and 4 and substituting into eqs 1 and 2, respectively, give

$$[AB] = \frac{[A][B]_0}{K_{dAB} + [A]} \quad (6)$$

$$[AC] = \frac{[A][C]_0}{K_{dAC} + [A]} \quad (7)$$

Substitution of [AB] and [AC] from eqs 6 and 7 into eq 5 and rearranging give

$$[A]^3 + a[A]^2 + b[A] - c[A]_0 = 0 \quad (8)$$

where

$$a = [B]_0 + [C]_0 + K_{dAB} + K_{dAC} - [A]_0$$

$$b = K_{dAC}[B]_0 + K_{dAB}[C]_0 + K_{dAB}K_{dAC} - [A]_0(K_{dAB} + K_{dAC})$$

$$c = K_{dAB}K_{dAC}$$

Equation 8 can be solved to give three solutions for [A]. The properties of the roots of the general cubic equation have been analyzed, and one has been identified as meaningful for this type of study (*29*):

$$2 \times \sqrt[6]{e} \times \cos\left\{\frac{1}{3}a \cos\left[\frac{-1}{2e}\left(\frac{27d + 2a^3 - 9ab}{27}\right)\right]\right\} - \frac{a}{3}$$

where

$$a = [B]_0 + [C]_0 + K_{dAB} + K_{dAC} - [A]_0 \text{ (as in eq 8)}$$

$$b = K_{dAC}[B]_0 + K_{dAB}[C]_0 + K_{dAB}K_{dAC} - K_{dAB}[A]_0 - K_{dAC}[A]_0 \text{ (as in eq 8)}$$

$$d = -([A]_0 K_{dAB} K_{dAC})$$

$$e = \frac{1}{4}\left(\frac{27d + 2a^3 - 9ab}{27}\right)^2 - \left[\frac{1}{4}\left(\frac{27d + 2a^3 - 9ab}{27}\right)^2 + \frac{1}{27}\left(\frac{3b - a^2}{3}\right)^3\right]$$

In the absence of a competitive ligand B, $[AC]_0$ formed is

$$[AC]_0 = \left([A]_0 + [C]_0 + K_{dAC} - \sqrt{([A]_0 + [C]_0 + K_{dAC})^2 - 4[C]_0[A]_0}\right)/2$$

In the case of the SPA, where A is the protein immobilized on a SPA bead and C is the radiolabeled protein, the observed signal (S) is linearly related to [AC] and no signals are obtained from species AB, A, B, or C. If S_{AC} is the signal of AC in the absence of B and S_{AB} is the signal when B is saturated with A

$$S = S_{AB} + (S_{AC} + S_{AB})\left(\frac{[AC]}{[AC]_0}\right)$$

The equations were entered into Grafit (version 5, Erithacus Software), which was used for nonlinear regression curve fitting.

Isothermal Titration Calorimetry (ITC)

ITC experiments were performed at 20 °C by injecting a sequence of thirty 10 μL aliquots of 70 μM Cdc42·GTP or mutant Cdc42·GTP into 1.4 mL of 7 μM ACK or ACK mutant solution in the sample cell of a Microcal MCS ITC instrument.

The experimental data were analyzed using Origin (Microcal). The end point of the titration was adjusted to zero before the resultant data were fitted to a binding isotherm describing binding at a single site (*30*). From the fit of the sigmoidal binding isotherm, values for the binding constant (K_a), the number of binding sites (n), and the enthalpy change (ΔH) were obtained.

Double Mutant Cycles

To calculate the coupling energy between the side chains of two residues expected to interact in a protein−protein interface, the residues were each mutated to alanine to remove the effects of the side chain. Substitution of alanine removes only side chain atoms past the β-carbon, unlike glycine, which would remove the entire side chain. Glycine, however, would introduce conformational flexibility into the mutant protein backbone, whereas alanine lacks the propensity to adopt unusual backbone dihedral angles and should retain the backbone conformation of the wild-type protein (*23*). The use of alanine also allows for conventional double mutant cycle analysis, whereas the use of non-alanine substitutions would require decomposition of the cycles (*31*, *32*). The values of the K_d for the interaction were obtained experimentally by SPA and ITC for each of the four possible

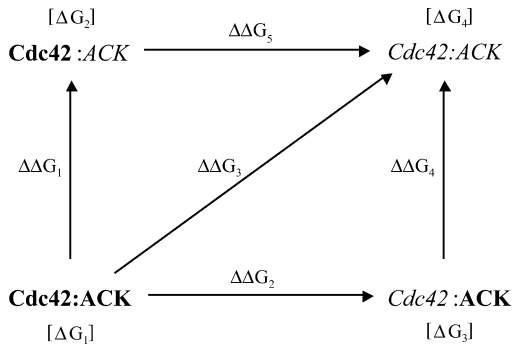

FIGURE 1: Double mutant cycle for Cdc42 and ACK. Proteins in bold are wild-type forms, and those in italics have been mutated. The Gibbs free energy is shown as ΔG and the change in the free energy of binding as $\Delta\Delta G$.

combinations of wild-type and mutant proteins. ΔG was then calculated for each experimental K_d value obtained, by convention in molar units, using eq 9, where R is the molar gas constant and T is the temperature in kelvin.

$$\Delta G = -RT \ln K_a = RT \ln K_d \quad (9)$$

For each possible combination of wild-type (bold) and mutant (italic) proteins ($\Delta G_{\mathbf{Cdc42-ACK}}$, $\Delta G_{\mathbf{Cdc42}-Cdc42-ACK}$, $\Delta G_{Cdc42-\mathbf{ACK}}$, and $\Delta G_{Cdc42-ACK}$), the mean and standard error of ΔG was calculated. A cycle was then constructed as shown in Figure 1, and the values for $\Delta\Delta G_{1-5}$ were calculated from ΔG for each interaction: $\Delta\Delta G_1 = \Delta G_{\mathbf{Cdc42}-ACK} - \Delta G_{\mathbf{Cdc42-ACK}}$, $\Delta\Delta G_2 = \Delta G_{Cdc42-\mathbf{ACK}} - \Delta G_{\mathbf{Cdc42-ACK}}$, $\Delta\Delta G_3 = \Delta G_{Cdc42-ACK} - \Delta G_{\mathbf{Cdc42-ACK}}$, $\Delta\Delta G_4 = \Delta G_{Cdc42-ACK} - \Delta G_{Cdc42-\mathbf{ACK}}$, and $\Delta\Delta G_5 = \Delta G_{Cdc42-ACK} - \Delta G_{\mathbf{Cdc42}-ACK}$. From Figure 1, $\Delta\Delta G_3 = \Delta\Delta G_1 + \Delta\Delta G_5 = \Delta\Delta G_2 + \Delta\Delta G_4$. Errors in $\Delta\Delta G_{1-5}$ and $\Delta\Delta G_{int}$ were calculated from the square root of the sum of the variance for each individual value of ΔG or $\Delta\Delta G$ used.

Theoretical Background

Consider a pair of residues that are proposed to directly interact across a protein−protein interface in which replacement of the side chains does not induce any structural changes in the proteins or the complex, other than loss of interaction between the two residues. In this situation, mutation of the second residue in the pair has no further effect than that of mutation of the first residue and $\Delta\Delta G_4 = \Delta\Delta G_5 = 0$. Also, $\Delta\Delta G_1 = \Delta\Delta G_2 = \Delta\Delta G_3$. The interaction energy (coupling energy) $\Delta\Delta G_{int}$ (*10*) is given by $\Delta\Delta G_{int} = \Delta\Delta G_4 - \Delta\Delta G_1 = \Delta\Delta G_5 - \Delta\Delta G_2 = \Delta G_{\mathbf{Cdc42-ACK}} + \Delta G_{Cdc42-ACK} - \Delta G_{\mathbf{Cdc42}-ACK} - \Delta G_{Cdc42-\mathbf{ACK}}$. Under circumstances where $\Delta\Delta G_4$ equals $\Delta\Delta G_5$, $\Delta\Delta G_3$ equals $\Delta\Delta G_{int}$. However, under other circumstances, the energy of the interaction cannot solely be attributed to the direct interactions between the side chains of the two residues, $\Delta\Delta G_4$ and $\Delta\Delta G_5$ may not be zero, and $\Delta\Delta G_{int}$ may not equal $\Delta\Delta G_1$, $\Delta\Delta G_2$, or $\Delta\Delta G_3$. $\Delta\Delta G_{int}$ can also be zero, in which case no interaction occurs between the side chains that contributes energetically to the overall protein−protein interaction. If $\Delta\Delta G_{int}$ is positive, then the simultaneous presence of both side chains actually destabilizes the Cdc42−ACK binary complex. Using the double mutant cycle analysis and associated equations (Figure 1), values for $\Delta\Delta G_{1-5}$ and $\Delta\Delta G_{int}$ were calculated for each pair of mutations.

RESULTS

Determination of Binding Constants for the Interaction between Wild-Type and Mutant Cdc42 and ACK

Double mutant analysis requires very precise determinations of K_d values, over a range that depends upon the magnitude of the effect of the mutations and in particular the double mutations being examined. To achieve this, we employed three different methods to measure K_d values in this study.

Isothermal titration calorimetry (ITC) detects the small amounts of heat absorbed or released by molecular interactions. It has been widely used for double mutant cycle analysis because it is a solution-based method, which, under appropriate conditions, gives precise "gold standard" K_d values. Additionally, the apparent stoichiometry is determined which establishes the functional integrity of the proteins and/or provides accurate estimation of their concentrations. From the same experiment, enthalpy and entropy data can also be obtained which can prove informative in interpreting the effects of mutations. Hence, we have used ITC wherever possible.

In principle, ITC can measure the binding constants over a wide range of affinities typically with a K_d of 1 nM to 1 mM. However, a key drawback of ITC is its relative insensitivity, and in practice, the available range of K_d values that can be measured can be much narrower. The accessible range is principally determined by the magnitude of the enthalpy change and the amount of protein available. Good quality curve fits are obtained where the system is set up such that $10 < c < 100$, where $c = [P]/K_d$ and [P] is the concentration of protein in the calorimeter cell. As an example, for a K_d of 5 μM, with a c of 30, a complete experiment (e.g., quadruplicate runs plus controls) requires 30 mg of Cdc42 protein and similar amounts of ACK. Additionally, it was found that, in the Cdc42 and ACK mutant studies, the higher concentrations required to measure very weak affinities gave imperfect data, probably due to aggregation−disaggregation effects during the titration.

For these reasons, this study also employed scintillation proximity assays (SPAs), which extend the range of accessible affinities. These methods have previously been shown to give comparable data on small G protein−effector binding as data measured by ITC (*25*, *33*). SPA relies on scintillation that occurs when wild-type or mutant [^{3}H]GTP·Cdc42 binds to a wild-type or mutant GST effector captured by anti-GST antibody on a protein A-coated SPA bead. K_d values were determined by SPA in two distinct ways.

In the direct binding mode, the concentration of radiolabeled Cdc42 was varied to obtain a binding isotherm, which is fitted to an appropriate 1:1 binding model. The weakest affinity that can be measured in this way is limited by the magnitude of the signal seen in control experiments in which the GST effector is omitted; typically, the maximum concentration that could be used was between 500 and 1500 nM, and hence, K_d values of >0.5 μM could not always be precisely determined. The direct binding method involves interaction between Cdc42 and an immobilized effector, so apparent K_d values are obtained, which are within 2- or 3-fold of those obtained from true solution measurements (see ref *34*).

In the competition mode, wild-type or mutant, GST-free ACK was titrated into assays containing a fixed concentration of wild-type or mutant [^{3}H]GTP·Cdc42 and a fixed concentration of wild-type GST effector. The free ACK competes with the GST effector for binding to [^{3}H]GTP·Cdc42. Here, the weakest affinity that could be measured was determined by the concentration of the competing ACK protein that could be used; in practice, trace contamination with GST limited the maximum concentration of ACK to 2−3 μM.

This study, like previous mutational analyses (*7*, *8*), used Q61L Δ7 Cdc42 and $ACK_{448-489}$. The Q61L mutation confers a significantly decreased intrinsic GTPase activity that allows Cdc42 complexed to GTP, rather than a GTP analogue, to be used in the binding measurements. Q61L Cdc42·GTP binds with a higher affinity than the wild-type Cdc42·GMPPNP (a nonhydrolyzable analogue of GTP) to the CRIB effector proteins ACK, PAK, and WASP and also to the regulator protein RhoGAP. However, there are no differences in effector specificity between the wild-type (wt) and Q61L Cdc42 proteins (*7*). The higher affinity of the Q61L mutant makes it particularly useful in the type of studies presented here as the additional mutations under investigation lead to dramatic decreases in affinity. The presence of the Q61L mutation therefore allows more accurate measurements of the low affinities. The Δ7 refers to deletion of the seven C-terminal amino acids, which we have found reduces the level of aggregation of the protein (*24*) and thus should decrease the errors in the K_d measurement, particularly those generated from ITC data. Cdc42 Δ7 Q61L is henceforth termed the wild type. The $ACK_{448-489}$ fragment used in these experiments binds Cdc42 with high affinity (*7*, *24*), and a similar fragment, $ACK_{443-495}$, has been demonstrated to bind Cdc42 with an affinity similar to that of full-length ACK (*4*).

Cdc42 L174A−ACK L449A Interaction

ITC. ITC was used to monitor the interactions between the four possible combinations of wild-type (wt) and mutant proteins: wt Cdc42−wt ACK, Cdc42 L174A−wt ACK, wt Cdc42−ACK L449A, and Cdc42 L174A−ACK L449A. An example of the raw ITC data is shown for the interaction between wt Cdc42·GTP and wt ACK in Figure 2, and the results of all the data analyses are summarized in Table 1. The measured stoichiometry (*N*) of the interaction between wt Cdc42·GTP and ACK L449A was close to 1:1 (Table 1), demonstrating that this mutant was active and at the correct concentration. The stoichiometry (*N*) of the interactions between Cdc42 L174A·GTP and ACK or ACK L449A was lower (0.7−0.8 mol of Cdc42/mol of ACK), suggesting that the concentration of Cdc42 L174A·GTP was actually slightly higher than expected. This difference does not significantly affect the K_d values obtained from these assays.

The ACK L449A mutation decreased the affinity of ACK for Cdc42·GTP 9-fold (Table 1), and the L174A mutation decreased the affinity of Cdc42 for ACK 12-fold (Table 1). The binding affinity of Cdc42 L174A for ACK L449A was reduced 23-fold, compared with that for the interaction between the two wild-type proteins.

The interaction between Cdc42·GTP and ACK was exothermic with a ΔH of −13 ± 2 kcal/mol, and the enthalpy change with either mutation or both was not significantly different (Table 1). The change in affinity with these mutations was driven instead by entropic changes as seen by the decrease in ΔS (Table 1).

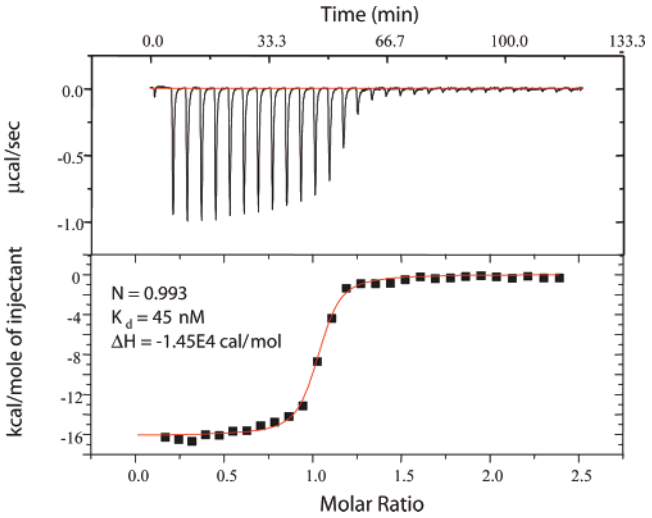

FIGURE 2: Isothermal titration calorimetry measurements of binding of wild-type Cdc42 to wild-type ACK. Cdc42 Q61L·GTP (70 μM) was titrated into 7 μM ACK, and heat changes were recorded continuously with time. The top panel shows the raw data from injections. The peaks were integrated to give the heat change associated with each injection, and a buffer control was subtracted. The resultant data are plotted in the bottom panel, as the molar ratio of Cdc42 injected into ACK against the heat output per mole of injected Cdc42. The line through the points is a least-squares fit to the data assuming a single-site binding model.

Direct Binding Assays by SPA. The results for SPA direct binding assays for the four possible combinations of wild-type and mutant proteins (wt Cdc42−wt ACK, Cdc42 L174A−wt ACK, wt Cdc42−ACK L449A, and Cdc42 L174A−ACK L449A) are shown in Figure 3 and Table 1.

The K_d of the wt Cdc42−ACK interaction of 25 ± 18 nM is consistent with the K_d obtained by Owen et al. (*7*) of 30 ± 4 nM for the interaction using this method. The errors in the values of the K_d are within the normal range for this assay system.

The L174A mutation decreased the affinity of Cdc42 for GST−ACK 30-fold (Figure 3A and Table 1), identical to the change we previously reported (*7*, *24*). The ACK L449A mutation decreased the affinity of ACK for Cdc42·GTP 11-fold (Figure 3B and Table 1). The affinity of mutant [^{3}H]-GTP·Cdc42 for mutant GST−ACK (Figure 3C) was reduced 125−180-fold, so these assays could no longer accurately measure it.

Competition SPAs. The results for SPA competition binding assays for the four possible combinations of wild-type and mutant proteins (wt Cdc42−wt ACK, Cdc42 L174A−wt ACK, wt Cdc42−ACK L449A, and Cdc42 L174A−ACK L449A) are shown in Figure 4 and Table 1.

The ACK L449A mutation decreased the affinity of ACK for Cdc42·GTP approximately 13-fold (Figure 4A and Table 1). The L174A mutation decreased the affinity of Cdc42 for ACK approximately 20-fold (Figure 4B and Table 1).

The binding of mutant [^{3}H]GTP·Cdc42 to mutant ACK (Figure 4B and Table 1) gave more reproducible values with the competition binding assay than with the direct binding assays. The Cdc42 L174A and ACK L449A mutations in combination decreased the affinity of the Cdc42−ACK

Table 1: K_d Values for the Interaction between Wild-Type and Mutant Cdc42·GTP and Wild-Type and Mutant ACK Proteins Determined by ITC, Direct Binding SPAs, and Competition SPAs[a]

	ITC				SPA (direct)	SPA (competition)
proteins	K_d (nM)	stoichiometry (N)	ΔH (kcal/mol)	ΔS (cal mol^{-1} K^{-1})	K_d (nM)	K_d (nM)
Cdc42-ACK	40 ± 8	1.1 ± 0.1	−13 ± 2	−10	25 ± 18	6 ± 1
Cdc42 L174A−**ACK**	480 ± 20	0.8 ± 0.1	−13 ± 1	−15	750 ± 330	130 ± 20
Cdc42−*ACK L449A*	360 ± 160	1.0 ± 0.2	−12 ± 3	−11	270 ± 15	85 ± 5
Cdc42 L174−*ACK L449A*	920 ± 230	0.7 ± 0.1	−13 ± 3	−16	3860 ± 950[b]	580 ± 26
Cdc42 V42A−**ACK**	1300 ± 70	1.2 ± 0.1	−17 ± 1	−31	280 ± 120	53 ± 12
Cdc42−*ACK I463A*	180 ± 20	1.0 ± 0.2	−12 ± 3	−10	110 ± 20	30 ± 12
Cdc42 V42A−*ACK I463A*	*c*	1.2 ± 0.1	−17 ± 8	not available	*d*	400 ± 50

[a] Proteins in bold are wild-type proteins; those in italics are mutated as indicated. Concentrations of protein used in ITC were 70 μM Cdc42·GTP and 7 μM ACK. Experiments were performed at 20 °C. Each value represents the mean ± standard deviation for three or four repeats of the assay. In the SPA experiments, each value represents the mean ± standard deviation for three repeats of the assay except for the double mutants where the values represent two repeats. [b] Individual values of K_d were 3190 and 4530 nM. [c] Individual values of K_d for *Cdc42 V42A*−*ACK I463A* were 1330, 1670, 4570, and 7940 nM. [d] K_d was not well-defined via curve fitting.

interaction 91-fold, which is greater than the effect of each individual mutation (13- and 20-fold, respectively).

Comparison of K_d Determinations by the Three Methods. A reliable determination of the K_d for the mutant Cdc42−mutant ACK interaction could not be obtained using SPA direct binding assays due to the low affinity but was obtained using the competition SPA and ITC. Therefore, both ITC and the competition SPA gave a complete set of the four K_d values required for the analysis. The reproducibility and errors in both were sufficiently good that a meaningful double mutant analysis could be undertaken.

For the double mutant analysis, the relative effects of mutation on affinity are relevant. The ACK L449A mutation resulted in decreases in affinity for wt Cdc42 of 11-, 13-, and 9-fold by direct SPA, competition SPA, and ITC, respectively. Similarly, the L174A mutation resulted in a decrease in affinity for wt ACK of 20- and 12-fold as determined by competition SPA and ITC, respectively; the decrease in affinity measured by direct SPA was ∼30-fold, but the errors in this ratio are high. The double mutation, Cdc42 L174A−ACK L449A, resulted in decreases in affinity of 91- and 23-fold by competition SPA and ITC, respectively. Thus, the relative effects of each mutant on K_d values obtained by the direct binding SPA, ITC, and competition SPA methods paralleled each other, although the numerical values of the K_d values differed, with ITC giving higher K_d values than direct binding SPA, which in turn were higher than those from competition SPA. The effect of the Cdc42 L174A−ACK L449A mutation is 3.9-fold less when measured by ITC than by SPA competition assay.

For this pair, therefore, double mutant analysis was performed both on ITC and on competition SPA data.

Double Mutant Cycle Thermodynamic Analysis. ΔG was separately calculated for each experimentally determined K_d obtained using the competition SPA. For each interacting pair, the mean ΔG and its standard error were then calculated (Table 2). These values were used to calculate $\Delta\Delta G_{1-5}$ and $\Delta\Delta G_{int}$ (the interaction energy between the two residues) and their associated errors, which are shown in Figure 5A.

For the interaction between Cdc42 Leu174 and ACK Leu449, $\Delta\Delta G_4$ and $\Delta\Delta G_5$ are similar in magnitude to $\Delta\Delta G_1$ and $\Delta\Delta G_2$. Thus, the loss of interaction between Cdc42 and ACK is roughly doubled in the double mutant ($\Delta\Delta G_3$) as compared with either mutation alone ($\Delta\Delta G_{1/2}$). $\Delta\Delta G_{int} = -600 \pm 106$ cal/mol, which is also much lower than $\Delta\Delta G_3$ (2650 ± 82 cal/mol). These data suggest that there is only a weak energetic contribution to the overall stability of the Cdc42−ACK complex through the direct interaction of Leu174 and Leu449 residues across the interface. In fact, the direct interaction between Cdc42 Leu174 and ACK Leu449 constitutes 23% of the energy lost when the two mutations are present in the complex.

A similar analysis of the K_d data obtained by ITC was performed. The ΔG values are summarized in Table 3, and values for $\Delta\Delta G_{1-5}$ and $\Delta\Delta G_{int}$ are shown in Figure 5B. Here $\Delta\Delta G_4$ and $\Delta\Delta G_5$ are much smaller than $\Delta\Delta G_1$ and $\Delta\Delta G_2$, and $\Delta\Delta G_3$ is closer to $\Delta\Delta G_1$ or $\Delta\Delta G_2$. For the interaction between Cdc42 Leu174 and ACK Leu449, $\Delta\Delta G_{int} = -870 \pm 231$ cal/mol when calculated from the ITC data, greater than that obtained by competition SPA, and the direct contribution between Cdc42 Leu174 and ACK Leu449 represents 50% of the energy lost when both mutations are present in the complex.

Overall, although it is less clear with the SPA data, there is a consistent, favorable, direct interaction between the side chains of these residues in these analyses, although a large proportion of the interaction may still be ascribed to other energetic effects.

Cdc42 V42A−ACK I463A Interaction

ITC. ITC was used to monitor the interactions between the four possible combinations of wild-type and mutant proteins (wt Cdc42−wt ACK, Cdc42 V42A−wt ACK, wt Cdc42−ACK I463A, and Cdc42 V42A−ACK I463A), and the analyses are summarized in Table 1. The measured stoichiometry (N) of interaction was close to 1:1 (Table 1), demonstrating that all proteins were active and at the correct concentrations.

The ACK I463A mutation decreased the affinity of ACK for Cdc42·GTP by approximately 5-fold (Table 1), whereas the V42A mutation decreased the affinity of Cdc42 for ACK by approximately 33-fold (Table 1). The binding affinity of Cdc42 V42A for ACK I463A was weaker still and could not be reliably determined by ITC.

The interaction between wt Cdc42 and ACK I463A was exothermic with a ΔH of −13 ± 2 kcal/mol and was not significantly different from the wt Cdc42−wt ACK interaction. The Cdc42 V42A−wt ACK interaction, however, exhibited a more favorable ΔH (−17 ± 1 kcal/mol), suggesting that removal of the Val42 side chain allowed a

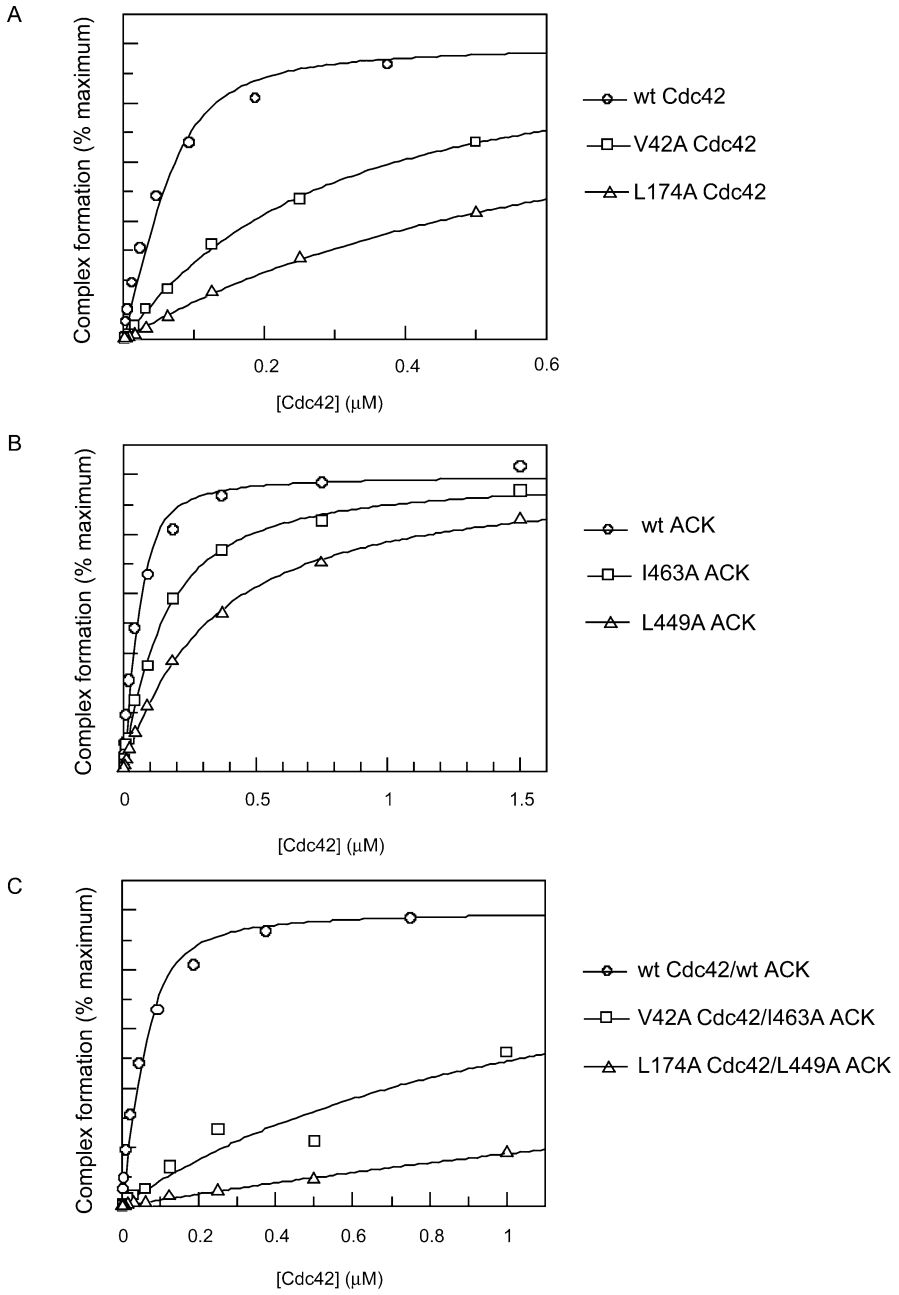

FIGURE 3: (A) Fits of [^{3}H]GTP·Cdc42 and [^{3}H]GTP·Cdc42 mutants binding to wild-type GST−ACK. The interaction with Cdc42 is shown with circles, with Cdc42 V42A as squares, and with Cdc42 L174A as triangles. (B) Fits of [^{3}H]GTP·Cdc42 binding to wild-type GST−ACK and GST−ACK mutant proteins. The interaction with wild-type ACK is shown as circles, with ACK I463A as squares, and with ACK L449A as triangles. (C) Fits of wild-type and mutant [^{3}H]GTP·Cdc42 proteins binding to wild-type GST−ACK and GST−ACK mutant proteins. The interaction of Cdc42 with ACK is shown as circles, the interaction of Cdc42 V42A with ACK I463A as squares, and the interaction of Cdc42 L174A with ACK L449A as triangles. The figures show complex formation as a percentage of a maximum in which each point has been normalized as a percentage of S_{max}, the maximum SPA signal when GST−ACK is fully complexed with [^{3}H]-GTP·Cdc42, from each independent fit.

more enthalpically favorable interaction to occur. The decrease in affinity is a result of a considerably larger change in ΔS (Table 1), suggesting that the removal of Val42 is entropically deleterious to the point where this compensates for the favorable enthalpic change.

Direct Binding Assessed by SPA. The results for SPA direct binding assays for the four possible combinations of wild-type and mutant proteins (wt Cdc42−wt ACK, Cdc42 V42A−wt ACK, wt Cdc42−ACK I463A, and Cdc42 V42A−ACK I463A) are shown in Figure 3 and Table 1.

The V42A mutation decreased the affinity of Cdc42 for GST−ACK approximately 11-fold (Figure 3A and Table 1), comparable to the effect of this mutation of 18-fold that we have shown previously (*24*). The ACK I463A mutation decreased the affinity for Cdc42·GTP approximately 4-fold (Figure 3B and Table 1). The affinity of Cdc42 V42A for GST−ACK I463A (Figure 3C and Table 1) was reduced such that it could not longer be accurately measured using this assay.

Competition SPA. The results for SPA competition binding assays for the four possible combination of wild-type and mutant proteins (wt Cdc42−wt ACK, Cdc42 V42A−wt ACK, wt Cdc42−ACK I463A, and Cdc42 V42A−ACK I463A) are shown in Table 1.

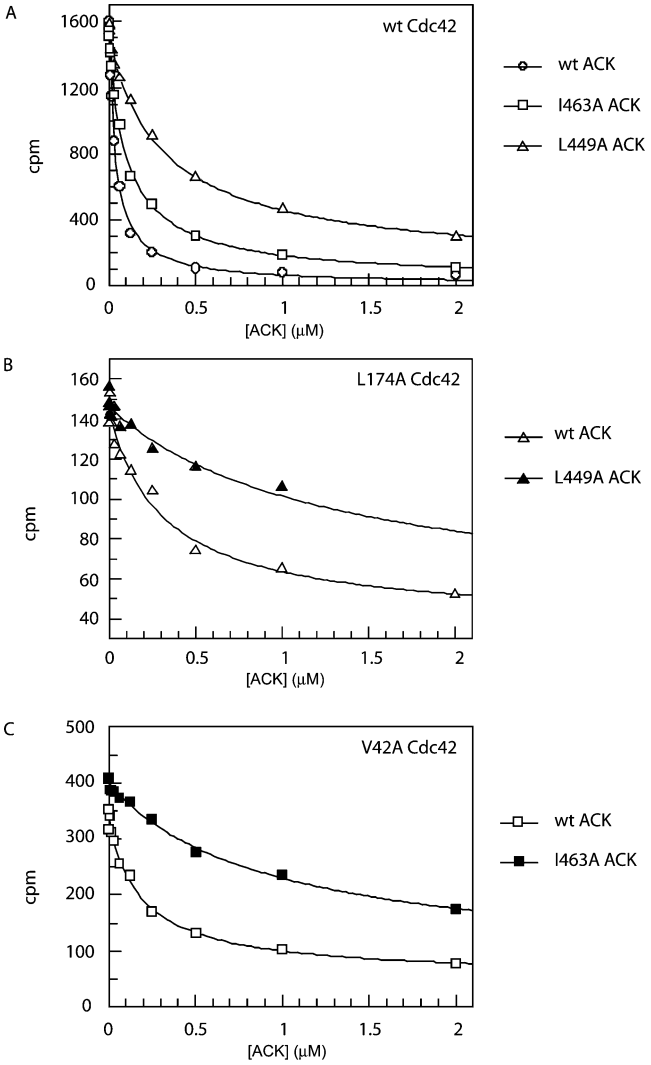

FIGURE 4: (A) Fits of wild-type ACK and ACK mutant fragment inhibition of the [^{3}H]GTP·Cdc42−GST-ACK interaction. Inhibition of the interaction by wild-type ACK is shown as circles, inhibition by ACK I463A as squares, and inhibition by ACK L449A as triangles. (B) Fits of wild-type ACK and ACK L449A fragment inhibition of the [^{3}H]GTP·Cdc42 L174A−GST-ACK interaction. Inhibition by ACK is shown as white squares and inhibition by ACK L449A as black squares. (C) Fits of wild-type ACK and ACK I463A fragment inhibition of the [^{3}H]GTP·Cdc42 V42A−GST-ACK interaction. Inhibition by ACK is shown as white triangles and inhibition by ACK I463A as black triangles.

Table 2: Calculation of ΔG_{1-4} Values for the Cdc42 L174A−ACK L449A Double Mutant from SPA Competition Assay Data

	interaction	K_d (nM)	ΔG (cal/mol)	mean ΔG (cal/mol)
ΔG_1	Cdc42−ACK	7	−10910	−10990 ± 80
		7	−10920	
		5	−11150	
ΔG_2	Cdc42−ACK L449A	81	−9500	−9480 ± 15
		86	−9470	
		88	−9460	
ΔG_3	Cdc42 L174A−ACK	110	−9310	−9250 ± 65
		140	−9180	
ΔG_4	Cdc42 L174A−ACK L449A	630	−8320	−8340 ± 20
		580	−8360	

The ACK I463A mutation decreased the affinity of ACK for Cdc42·GTP approximately 5-fold (Figure 4A and Table 1). The V42A mutation decreased the affinity of Cdc42 for ACK approximately 8-fold (Figure 4C and Table 1).

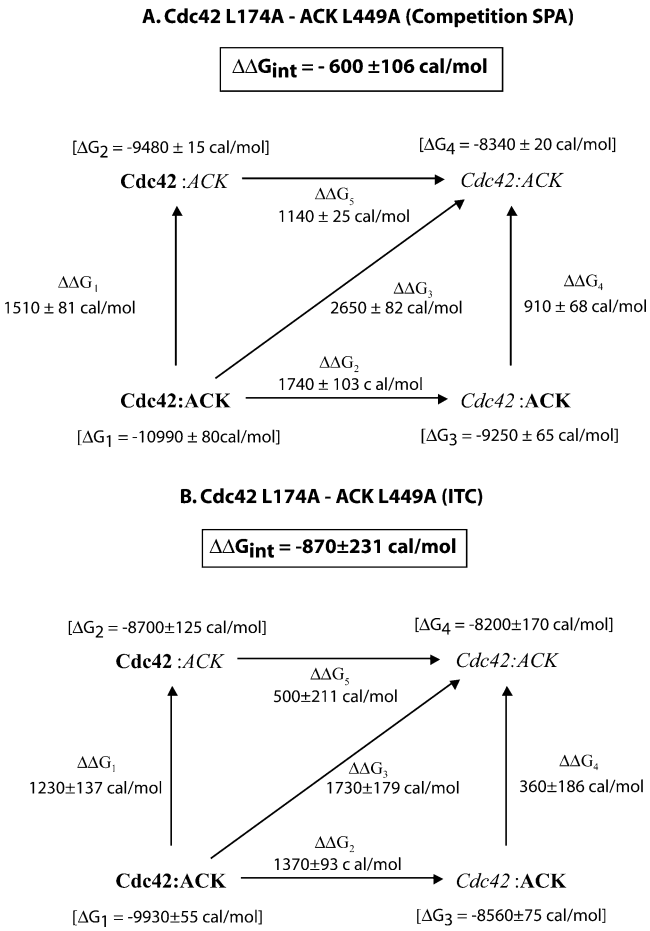

FIGURE 5: (A) Energy of interaction ($\Delta\Delta G_{int}$) of Cdc42 Leu174 with ACK Leu449 as determined from competition SPA data. The ΔG was determined for each pair of proteins using the measured K_d ($\Delta G = RT \ln K_d$) and used to calculate the change in free energy ($\Delta\Delta G$) associated with the introduction of each individual or pair of mutations. These values were then used as described to calculate $\Delta\Delta G_{int}$ (where $\Delta\Delta G_{int} = \Delta\Delta G_3 - \Delta\Delta G_2 - \Delta\Delta G_1$). (B) Energy of interaction of Cdc42 Leu174 with ACK Leu449 as determined from ITC data. Values were calculated as described for panel A.

Table 3: Calculation of ΔG_{1-4} Values for the Cdc42 L174A−ACK L449A Double Mutant from ITC Data

	interaction	K_d (nM)	ΔG (cal/mol)	mean ΔG (cal/mol)
ΔG_1	Cdc42−ACK	45	−9850	−9930 ± 55
		35	−10000	
		47	−9830	
		31	−10060	
ΔG_2	Cdc42−ACK L449A	200	−9000	−8700 ± 125
		300	−8800	
		550	−8400	
		400	−8600	
ΔG_3	Cdc42 L174A−ACK	480	−8470	−8560 ± 75
		460	−8490	
		320	−8700	
ΔG_4	Cdc42 L174A−ACK L449A	340	−8700	−8200 ± 170
		1240	−7900	
		1100	−80020	
		780	−8200	

The binding of Cdc42 V42A to ACK I463A (Figure 4C) gave more reproducible data with the competition binding assay than with the direct binding assay, due to the extremely low affinities gained in the direct binding SPAs. The Cdc42 V42A−ACK I463A double mutation decreased the affinity of the Cdc42−ACK interaction by 63-fold, which is much

Table 4: Calculation of ΔG_{1-4} Values for the Cdc42 V42A−ACK I463A Double Mutant from SPA Competition Assay Data

	interaction	K_d (nM)	ΔG (cal/mol)	mean ΔG (cal/mol)
ΔG_1	Cdc42−ACK	7	−10910	−10990 ± 80
		7	−10920	
		5	−11150	
ΔG_2	Cdc42−ACK I463A	23	−10250	−10120 ± 125
		23	−10240	
		44	−9860	
ΔG_3	Cdc42 V42A−ACK	44	−9860	−9770 ± 95
		61	−9670	
ΔG_4	Cdc42 V42A−ACK I463A	370	−8620	−8570 ± 55
		440	−8520	

larger than the effect of the sum of the two individual mutations (8- and 5-fold).

Comparison of K_d Determinations by the Three Methods. A reliable determination of the K_d values for the Cdc42 V42A−ACK I463A interaction could not be obtained by either ITC or SPA direct binding assays but was obtained using the competition SPA. Therefore, only the competition SPA gave a complete set of the four K_d values required for the analysis. The reproducibility and errors in the competition SPA were sufficiently good that a meaningful double mutant analysis could be undertaken. For this pair, double mutant analysis was therefore performed on only competition SPA data.

The data obtained by the direct binding SPA and ITC could, however, be used to validate data obtained from the competition SPA. Comparison of data with the two SPAs (Table 1) shows that the competition SPA gives K_d values lower than those from the direct binding SPA, but the relative effects of each mutation are similar. Numerically, the K_d values obtained from ITC (Table 1) are also higher than those obtained from the competition SPA (Table 1). With the wt Cdc42−ACK 1519A pair, ITC, direct SPA, and competition SPA gave the same relative effects of the I463A mutation (4−5-fold decrease in affinity). In contrast, with the Cdc42 V42A−wt ACK pair, the direct and competition SPAs showed an 11- and 8-fold decrease in affinity, respectively, whereas ITC showed a 33-fold decrease.

Double Mutant Cycle Thermodynamic Analysis. As previously, ΔG and the mean and standard error of ΔG were calculated from the values of K_d measured experimentally for each pair of interactions (Table 4). $\Delta\Delta G_{1-5}$ and $\Delta\Delta G_{int}$ values and their associated errors are shown in Figure 6.

For the interaction between Cdc42 Val42 and ACK Ile463, $\Delta\Delta G_4$ and $\Delta\Delta G_5$ are larger than or comparable to $\Delta\Delta G_1$ and $\Delta\Delta G_2$, so $\Delta\Delta G_3 \gg \Delta\Delta G_1$ or $\Delta\Delta G_2$. The loss of interaction between Cdc42 and ACK is more than doubled in the double mutant as compared with either mutation alone. $\Delta\Delta G_{int} = +320 \pm 185$ cal/mol. The error (σ) in $\Delta\Delta G_{int}$ is however high and is outside the 95% confidence limits of 2σ. This illustrates one of the disadvantages of the double mutant cycle method of analysis, where errors are accumulated by summing data from different mutations, thereby compounding the associated errors (as discussed in ref *20*). These data suggest that there is no favorable energetic contribution to the overall stability of the Cdc42−ACK complex through the direct interaction between Val42 and Ile463 residues across the interface. Furthermore, the positive value of $\Delta\Delta G_{int}$ implies that the interaction between the side chains of both residues across the interface may even be slightly unfavorable or destabilize the interaction between the two proteins.

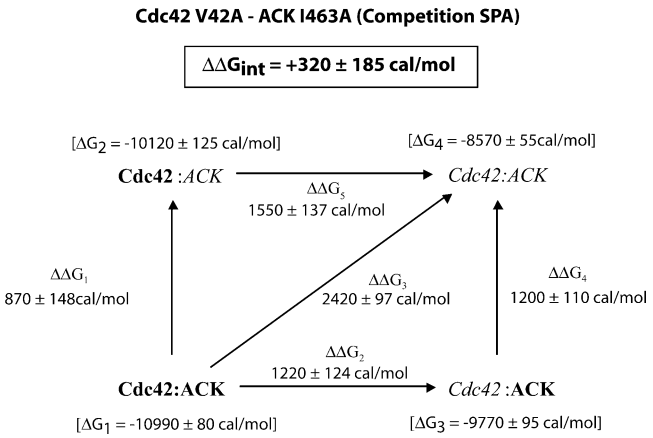

FIGURE 6: Energy of interaction of Cdc42 Val42 with ACK Ile463 as determined from competition SPA data. Values were calculated as described in the legend of Figure 5A.

DISCUSSION

When the effects of a single mutation in a protein−protein interface are analyzed, it is difficult to separate the contribution of breaking one specific interaction from that of removal of the interaction of the residue with other parts of the protein and also from structural reorganization. However, when double mutant cycle analysis is used, the interaction energies of each residue with the rest of the protein and solvent and the possible reorganization energies (ΔG_{reorg}) resulting from the mutations will cancel to leave just the interaction energies between the two residues. This is because each mutation is made both separately and in the presence of the other mutation (see Figure 1). This ideal situation has been frequently observed for mutations in proteins which do not show major rearrangements or conformational changes and where indeed the residue mutated only significantly interacts with the other partner residue (*16*, *20*, *35*, *36*). However, in other situations, the effects of mutation of each residue are not independent and isolated. In these cases, the reduction of interaction energy caused by removal of a side chain of one interacting residue is not equal to the decrease in interaction energy caused by removal of the side chain of the interacting partner residue.

The study presented here describes a double mutant cycle analysis of two specific hydrophobic interactions proposed, on the basis of the three-dimensional structure, to occur across the largely hydrophobic Cdc42−ACK interface. This analysis has a more general significance beyond these proteins for two key reasons. First, the energetics of hydrophobic interactions in protein−protein interfaces are relatively poorly studied. Second, both interacting proteins are known to undergo conformational changes when the protein−protein interface forms. In Cdc42, the effector binding loop (switch I) becomes structured, which may well impact the juxtaposed Val42, whereas the ACK GBD is conformationally flexible or unfolded structure in the free form and becomes structured on binding Cdc42 (*24*).

Double mutant cycle analysis requires precise K_d values for the four different possible interactions of wt and mutant proteins. More strictly, the requirement is for accurate relative

K_d values, as systematic differences will offset each other in the final analysis. Hence, we have employed several methods, which had the advantage of increasing our confidence in the results. Traditional ITC methods were used initially; however, it was not possible for us to use ITC to analyze the weaker interactions because of the high protein resource required and heat artifacts caused by aggregation at the necessarily high protein concentrations. Using SPA methodology, quantitative data could be obtained for all possible interactions. Although direct binding SPA data were not utilized for double mutant analysis data as results for the mutant−mutant interactions could not be obtained, we have included the data, partly as validation of the affinity data obtained by the other methods and also as the K_d values derived from direct SPAs were used in the calculation of K_d values from competition SPAs. In general, there was good agreement between the relative affinities obtained by the three methods, with the exception of the V42A mutation in Cdc42, which exhibited a larger loss of interaction energy with ACK when measured by ITC than by SPA.

The affinity of the wild-type Cdc42−ACK interaction calculated from the SPA competition assay was ~4-fold higher that that measured by direct SPA binding and ~6-fold higher than that measured using ITC. These variations, no doubt, result from inherent differences in these assays and their fitting methods, together with the assumptions and approximations made. ITC is a true solution method requiring few assumptions for calculation of K_d. In the direct binding SPA, the K_d is obtained from interaction between Cdc42 and GST−ACK immobilized on beads, requiring assumptions regarding the equivalence of GST−ACK and the effect of immobilization [both previously discussed (*34*)]. In the competition assay, the inhibitory interaction is between soluble ACK and soluble Cdc42 but the derived K_d is also dependent upon assumptions about the affinity of immobilized GST−ACK and Cdc42 in solution.

Double mutant analysis of the interaction between Cdc42 Leu174 and ACK Leu449 (Figure 5A,B) showed a small negative coupling energy ($\Delta\Delta G_{int}$): using SPA this was -0.6 ± 0.1 kcal/mol, while using ITC, it was -0.87 ± 0.23 kcal/mol. For both values, there >95% confidence that they significantly differ from zero. These negative coupling energies indicate that the interaction between Cdc42 Leu174 and ACK Leu449 contributes to the stabilization of the Cdc42−ACK interaction via the direct interaction of their side chains.

On the basis of the data, we conclude that while there is an energetic contribution to complex formation caused by the interaction between Leu174 of Cdc42 and Leu449 of ACK across the interface, a proportion of the total energy of the interaction ($\Delta\Delta G_3$) occurs through other factors. These might be due to interaction of these residues with other residues on the partner protein or due to intramolecular interactions resulting in stabilizing conformational effects in either the ground state of the individual partners or the complex.

It had been predicted from the Cdc42−ACK structure (*24*) that the direct interaction of the side chains of these two residues would be the major contact made by each residue across the interface. However, when a hydrophobic residue becomes buried in an interface, its whole surface area will be able to make hydrophobic contacts with residues around it. It would seem likely that this could potentially involve several residues across the interface. This differs from hydrophilic interactions such as salt bridges or hydrogen bonds, where a directional interaction is made by an individual group of a side chain. It is therefore likely that these residues make a patchwork of interactions with several residues across the interface. From the Cdc42−ACK structure (*24*; PDB entry 1cf4), it appears that Leu174 of Cdc42 makes its major contacts with Leu449 of ACK. However, its side chain interacts with the methyl group of Ala451 and is also close to the backbone of Ser450. Leu174 is on the C-terminal α-helix of Cdc42 and therefore also contacts the side chains of Glu171, Ile173, and Leu177, which are on the same face of the helix. The side chain of Leu449 of ACK on the other hand points into a pocket that is lined by these residues. Thus, there are several candidate residues that can participate in patch interactions in this region.

Double mutant cycle analysis for Cdc42 Val42 and ACK Ile463, using the SPA competition assay data, gives a coupling energy, $\Delta\Delta G_{int}$, for this combination of residues of $+0.32 \pm 0.18$ kcal/mol. Thus, the interaction between Val42 of Cdc42 and Ile463 of ACK provides no favorable energetic contribution to the complex and actually seems to have a small destabilizing effect on the Cdc42−ACK interaction. Although the interpretation that these residues are making a counterproductive interaction is the most straightforward interpretation of our data, an unfavorable interaction, however, between these two hydrophobic residues seems unlikely, unless there is a steric effect. Removal of either residue individually results in an increase in K_d, which implies loss of a favorable interaction. This is not compatible with a steric hindrance effect unless these residues are making favorable contacts with surrounding residues that have greater magnitude and therefore mask an unfavorable interaction between these two residues. The effect of the double mutation on the ΔG and K_d values of the Cdc42−ACK interaction is actually greater than the sum of the effects of the two single mutations (Tables 1, 2, and 5 and Figure 6) This is an example of superadditivity (*37*, *38*), a phenomenon that has been seen in other protein−protein interactions and can be used to classify interaction hot spots. These data together therefore imply that there are likely to be additional processes occurring in the double mutant. Since the regions involved in interaction are relatively flexible in both proteins, these could include structural rearrangements in the interface. Previously, we have presented an extensive analysis of the effects of Cdc42 mutations on the interaction with ACK that support the idea of structural rearrangements occurring after mutation of interface residues (*8*). It therefore seems probable that the outcome of the double mutant analysis results from compensatory structural effects within the interface. For example, structural rearrangements may, to an extent, compensate for the effect of the individual mutations, where removing a residue in the interface could create a cavity. As the maximum change in energy occurs when a mutation results in a full-sized empty cavity (*39*), it would be energetically more favorable for the structure of this complex to collapse to fill this space, with correspondingly smaller changes in energy for that mutation. However, when both mutations are made together, the cavity that is formed may be too large to be compensated to the same extent, resulting in greater destabilization of the complex.

This could then manifest as an unfavorable interaction in double mutant cycle analysis. A close inspection of the Cdc42−ACK structure reveals that Val42 could potentially form contacts with Phe462 as well as Ile463 and that Ile463 could form contacts with Thr43 and Ala41. The latter two residues, along with Val42, were among seven residues whose mutation in Rac was sufficient to change its affinity for ACK from nonmeasurable by SPA to 25 nM (*8*). In fact, structural rearrangements are not strictly necessary to explain these effects, as water molecules have been observed to fill a cavity caused by mutation (i.e., solvent rearrangements) in an antigen−antibody complex, resulting in a smaller effect on energetic parameters (*40*).

For a hydrophobic interaction, the thermodynamic analysis of the burial of a hydrophobic residue within a protein−protein interface (or in the core of a protein) is analogous to the transfer of that side chain from water to a hydrophobic solvent (*39*). In addition to the change in free energy from interaction with other residues when a hydrophobic residue is buried within the protein−protein interface, the ΔG terms will also include interaction energies of the residue with the rest of the protein and solvent, and possible reorganization energies.

ITC analysis of protein−protein interactions also gives a direct measure of ΔH in a system. ΔH for the interaction between Cdc42 and ACK remains constant for the L174A/L449A mutant combinations. Therefore, for this interaction, changes in the free energy in the system must be due to entropic effects, which is not surprising since we were attempting to disrupt hydrophobic contacts.

Although in ideal situations reorganization energy terms will offset each other in double mutant cycle analysis (*9*), it is unclear whether the relatively high flexibility of both proteins in this study will result in different reorganization energies for the different mutations and combinations of mutations. The relatively high errors found, in particular for the double mutants, and the positive value of $\Delta\Delta G_{int}$ calculated for the Cdc42 Val42−ACK Ile463 interaction from competition SPA data may imply structural rearrangements and collapse of the cavity formed upon removal of residue side chains on mutation to alanine. In this case, the thermodynamics of the effects of the mutations will be very complex and difficult to interpret. It would therefore be of interest to confirm whether the structures of these mutant complexes are the same as the wild-type complex.

Some recent work analyzing the complex between Cdc42 and the CRIB effector WASP (a member of the same effector family as ACK), using single-molecule dynamics, presented data to indicate that this interaction proceeded via a loosely bound semifolded intermediate of the effector, which then folded to the native binding state via interactions with Cdc42 (*41*, *42*). A similar mechanism of coupled folding and binding for intrinsically disordered proteins has recently been demonstrated for the CREB−CBP complex (*43*). Wang et al. (*41*) defined residues on both Cdc42 and WASP that are postulated to be the nucleation seeds for binding. These residues are Phe37 and Phe56 of Cdc42 and Leu263 and Leu267 of WASP. These may well mimic the types of hydrophobic interactions now thought to drive protein folding (*44*). In fact, it is possible that these types of interactions where both partners are unstructured will necessarily be predominantly hydrophobic to allow coupled folding and binding. The hydrophobic interactions would drive the initial folding event; however, as we show here, the Cdc42−ACK complex studied is driven by enthalpy not entropy so H bonds and ionic interactions are likely to be stabilizing the final complex. For the Cdc42−ACK complex, the interactions between Asp38 on Cdc42 and the two conserved His residues of the CRIB motif in ACK are likely candidates (*24*). The studies by Wang et al. again highlight the inherent flexibility of the small G protein−CRIB effector interactions and support our conclusions about the difficulty of interpreting double mutant cycle analysis data in these systems. The two residues on WASP defined as potential nucleation seeds in the Cdc42−WASP complex are not analogous to the residues that we have studied in ACK. In fact, the WASP residues lie in or near the helix of WASP (*45*), which is absent in ACK. It is tempting to speculate that this small region of secondary structure in the WASP GBD, evidence of which is also found in the free WASP fragment (*46*), is involved in the initial recognition stages of complex formation. This presents a dilemma with the Cdc42−ACK complex as free ACK has no secondary structural elements in the free form and indeed only forms a short β-strand in the complex with Cdc42, in which Ile463 resides. The two Cdc42 residues highlighted in the WASP study were Phe37 and Phe56. Phe37 forms part of switch I, which is a flexible loop on the surface of Cdc42, which becomes fixed only on interaction with its effectors. Phe56 is an unexpectedly crucial residue in Cdc42 for CRIB effector binding. In the Cdc42−WASP complex, it is identified as a residue that contacts the effector, explaining its role as a potential nucleation seed (*45*). We also identified Phe56 as a crucial residue for Cdc42−ACK binding; however, in this case, the contribution was unexpected, as Phe56 does not appear to be a contact residue. Instead, it is thought to pack behind switch 1, maintaining the switch in a conformation that is competent to interact with ACK (*8*), again indicating the importance of the protein conformation for these interactions.

The aim of this work was to confirm whether the stabilizing effect of Val42 and Leu174 in Cdc42 on its interaction with its effector protein ACK was due to direct pairwise interactions with Ile463 and Leu449 of ACK, respectively. In both cases, the predictions from the structure seem oversimplified. The interaction between Val42 of Cdc42 and Ile463 of ACK seems to be overshadowed by other interactions made by both residues, while the interaction between Leu174 of Cdc42 and Leu449 of ACK does contribute to the stabilizing effect of Leu174; however, these residues also seem to make significant secondary interactions.

Conclusions from this study, therefore, indicate that, to be effective, small molecule therapeutics directed against, e.g., Cdc42 Leu174, would need either to shield the whole of the exposed surface area of this side chain or to affect the conformational states in either the free or complexed form, rather than merely abrogating one specific interaction. Such information should be valuable in rationally developing therapeutic agents that abrogate protein−protein interactions via hydrophobic interfaces with conformationally flexible partners.

ACKNOWLEDGMENT

We thank Prof. Ed Manser, Prof. Louis Lim, and Mr. Gladstone Thompson for the constructs expressing GST−

ACK and GST−PAK, respectively, and Dr. Annie Bligh for providing the Grafit equations for analysis of competitive inhibition. We are also grateful to Prof. Ernest Laue and Dr. Steve McLaughlin for critical reading of the manuscript and helpful suggestions.

REFERENCES

1. Jaffe, A. B., and Hall, A. (2005) Rho GTPases: Biochemistry and Biology, *Annu. Rev. Cell Dev. Biol. 21*, 247−269.
2. Bishop, A. L., and Hall, A. (2000) Rho GTPases and their effector proteins, *Biochem. J. 348*, 241−255.
3. Owen, D., and Mott, H. R. (2005) Structural Analysis of Rho Protein Complexes, in *Protein and Cell Regulation (Rho Family GTPases)* (Manser, E., Ed.) pp 31−72, Kluwer Academic Publishers, Dordrecht, The Netherlands.
4. Manser, E., Leung, T., Salihuddin, H., Tan, L., and Lim, L. (1993) A Nonreceptor Tyrosine Kinase That Inhibits the GTPase Activity of p21(Cdc42), *Nature 363*, 364−367.
5. Eisenmann, K. M., McCarthy, J. B., Simpson, M. A., Keely, P. J., Guan, J. L., Tachibana, K., Lim, L., Manser, E., Furcht, L. T., and Iida, J. (1999) Melanoma chondroitin sulphate proteoglycan regulates cell spreading through Cdc42, Ack-1 and p130(cas), *Nat. Cell Biol. 1*, 507−513.
6. Teo, M., Tan, L., Lim, L., and Manser, E. (2001) The tyrosine kinase ACK1 associates with clathrin-coated vesicles through a binding motif shared by arrestin and other adaptors, *J. Biol. Chem. 276*, 18392−18398.
7. Owen, D., Mott, H. R., Laue, E. D., and Lowe, P. N. (2000) Residues in Cdc42 that specify binding to individual CRIB effector proteins, *Biochemistry 39*, 1243−1250.
8. Elliot-Smith, A. E., Mott, H. R., Lowe, P. N., Laue, E. D., and Owen, D. (2005) Specificity Determinants on Cdc42 for Binding Its Effector Protein ACK, *Biochemistry 44*, 12373−12383.
9. Fersht, A. R., Matouschek, A., and Serrano, L. (1992) The Folding of an Enzyme. 1. Theory of Protein Engineering Analysis of Stability and Pathway of Protein Folding, *J. Mol. Biol. 224*, 771−782.
10. Carter, P., Winter, G., Wilkinson, A. J., and Fersht, A. R. (1984) The use of double mutants to detect structural changes in the active site of tyrosyl-tRNA synthetase (*Bacillus stearothermophilus*), *Cell 38*, 835−840.
11. Serrano, L., Horovitz, A., Avron, B., Bycroft, M., and Fersht, A. R. (1990) Estimating the Contribution of Engineered Surface Electrostatic Interactions to Protein Stability By Using Double-Mutant Cycles, *Biochemistry 29*, 9343−9352.
12. Tissot, A. C., Vuilleumier, S., and Fersht, A. R. (1996) Importance of two buried salt bridges in the stability and folding pathway of barnase, *Biochemistry 35*, 6786−6794.
13. Matouschek, A., Kellis, J. T., Serrano, L., Bycroft, M., and Fersht, A. R. (1990) Transient Folding Intermediates Characterized By Protein Engineering, *Nature 346*, 440−445.
14. Stenberg, G., Dragani, B., Cocco, R., Mannervik, B., and Aceto, A. (2000) A conserved "hydrophobic staple motif" plays a crucial role in the refolding of human glutathione transferase P1-1, *J. Biol. Chem. 275*, 10421−10428.
15. Vaughan, C. K., Harryson, P., Buckle, A. M., and Fersht, A. R. (2002) A structural double-mutant cycle: Estimating the strength of a buried salt bridge in barnase, *Acta Crystallogr. D58*, 591−600.
16. Schreiber, G., and Fersht, A. R. (1995) Energetics of Protein-Protein Interactions: Analysis of the Barnase-Barstar Interface By Single Mutations and Double Mutant Cycles, *J. Mol. Biol. 248*, 478−486.
17. Frisch, C., Schreiber, G., Johnson, C. M., and Fersht, A. R. (1997) Thermodynamics of the interaction of barnase and barstar: Changes in free energy versus changes in enthalpy on mutation, *J. Mol. Biol. 267*, 696−706.
18. Albeck, S., Unger, R., and Schreiber, G. (2000) Evaluation of direct and cooperative contributions towards the strength of buried hydrogen bonds and salt bridges, *J. Mol. Biol. 298*, 503−520.
19. Ackermann, E. J., Ang, E. T. H., Kanter, J. R., Tsigelny, I., and Taylor, P. (1998) Identification of pairwise interactions in the α-neurotoxin-nicotinic acetylcholine receptor complex through double mutant cycles, *J. Biol. Chem. 273*, 10958−10964.
20. Pons, J., Rajpal, A., and Kirsch, J. F. (1999) Energetic analysis of an antigen/antibody interface: Alanine scanning mutagenesis and double mutant cycles on the HyHEL-10/lysozyme interaction, *Protein Sci. 8*, 958−968.
21. Berggrun, A., and Sauer, R. T. (2000) Interactions of Arg2 in the Mnt N-terminal arm with the central and flanking regions of the mnt operator, *J. Mol. Biol. 301*, 959−973.
22. Adams, H., Blanco, J. L. J., Chessari, G., Hunter, C. A., Low, C. M. R., Sanderson, J. M., and Vinter, J. G. (2001) Quantitative determination of intermolecular interactions with fluorinated aromatic rings, *Chem.−Eur. J. 7*, 3494−3503.
23. Morrison, K. L., and Weiss, G. A. (2001) Combinatorial alanine-scanning, *Curr. Opin. Chem. Biol. 5*, 302−307.
24. Mott, H. R., Owen, D., Nietlispach, D., Lowe, P. N., Manser, E., Lim, L., and Laue, E. D. (1999) Structure of the small G protein Cdc42 bound to the GTPase-binding domain of ACK, *Nature 399*, 384−388.
25. Thompson, G., Owen, D., Chalk, P. A., and Lowe, P. N. (1998) Delineation of the Cdc42/Rac-binding domain of p21-activated kinase, *Biochemistry 37*, 7885−7891.
26. Rittinger, K., Walker, P. A., Eccleston, J. F., Nurmahomed, K., Owen, D., Laue, E., Gamblin, S. J., and Smerdon, S. J. (1997) Crystal structure of a small G protein in complex with the GTPase-activating protein RhoGAP, *Nature 388*, 693−697.
27. Graham, D. L., Eccleston, J. F., Chung, C. W., and Lowe, P. N. (1999) Magnesium fluoride-dependent binding of small G proteins to their GTPase-activating proteins, *Biochemistry 38*, 14981−14987.
28. Bligh, S. W. A., Haley, T., and Lowe, P. N. (2003) Measurement of dissociation constants of inhibitors binding to Src SH2 domain protein by non-covalent electrospray ionization mass spectrometry, *J. Mol. Recognit. 16*, 139−147.
29. Wang, Z. X. (1995) An Exact Mathematical Expression for Describing Competitive-Binding of Two Different Ligands to a Protein Molecule, *FEBS Lett. 360*, 111.
30. Wiseman, T., Williston, S., Brandts, J. F., and Lin, L. N. (1989) Rapid Measurement of Binding Constants and Heats of Binding Using a New Titration Calorimeter, *Anal. Biochem. 179*, 131−137.
31. Faiman, G. A., and Horovitz, A. (1996) On the choice of reference mutant states in the application of the double-mutant cycle method, *Protein Eng. 9*, 315−316.
32. Horovitz, A. (1996) Double-mutant cycles: A powerful tool for analyzing protein structure and function, *Folding Des. 1*, R121−R126.
33. Lawton, D. G., Gorman, C., and Lowe, P. N. (1997) Small G protein characterisation by iosothermal titration calorimetry, *Biochem. Soc. Trans. 25*, 510S.
34. Graham, D. L., Eccleston, J. F., and Lowe, P. N. (1999) The conserved arginine in Rho-GTPase-activating protein is essential for efficient catalysis but not for complex formation with Rho GDP and aluminum fluoride, *Biochemistry 38*, 985−991.
35. Goldman, E. R., DallAcqua, W., Braden, B. C., and Mariuzza, R. A. (1997) Analysis of binding interactions in an idiotope-antiidiotope protein-protein complex by double mutant cycles, *Biochemistry 36*, 49−56.
36. Kiel, C., Serrano, L., and Herrmann, C. (2004) A detailed thermodynamic analysis of Ras/effector complex interfaces, *J. Mol. Biol. 340*, 1039−1058.
37. Chen, C. Z., and Shapiro, R. (1999) Superadditive and subadditive effects of "hot spot" mutations within the interfaces of placental ribonuclease inhibitor with angiogenin and ribonuclease A, *Biochemistry 38*, 9273.
38. Shapiro, R., Ruiz-Gutierrez, M., and Chen, C. Z. (2000) Analysis of the interactions of human ribonuclease inhibitor with angiogenin and ribonuclease A by mutagenesis: Importance of inhibitor residues inside versus outside the C-terminal "hot spot", *J. Mol. Biol. 302*, 497.
39. Fersht, A. R., Jackson, S. E., and Serrano, L. (1993) Protein Stability: Experimental Data from Protein Engineering, *Philos. Trans. R. Soc. London, Ser. A 345*, 141.
40. Dall'Acqua, W., Goldman, E. R., Lin, W. H., Teng, C., Tsuchiya, D., Li, H. M., Ysern, X., Braden, B. C., Li, Y. L., Smith-Gill, S. J., and Mariuzza, R. A. (1998) A mutational analysis of binding interactions in an antigen-antibody protein-protein complex, *Biochemistry 37*, 7981−7991.
41. Wang, J., Lu, Q., and Lu, H. P. (2006) Single-molecule dynamics reveal cooperative binding-folding in protein recognition, *PLoS Comput. Biol. 2*, 842−852.
42. Tan, X., Nalbant, P., Toutchkine, A., Hu, D. H., Vorpagel, E. R., Hahn, K. M., and Lu, H. P. (2004) Single-molecule study of

protein-protein interaction dynamics in a cell signaling system, *J. Phys. Chem. B 108*, 737−744.
43. Sugase, K., Dyson, H. J., and Wright, P. E. (2007) Mechanism of coupled folding and binding of an intrinsically disordered protein, *Nature 447*, 1021.
44. Dyson, H. J., Wright, P. E., and Scheraga, H. A. (2006) The role of hydrophobic interactions in initiation and propagation of protein folding, *Proc. Natl. Acad. Sci. U.S.A. 103*, 13057−13061.
45. Abdul-Manan, N., Aghazadeh, B., Liu, G. A., Majumdar, A., Ouerfelli, O., Siminovitch, K. A., and Rosen, M. K. (1999) Structure of Cdc42 in complex with the GTPase-binding domain of the 'Wiskott-Aldrich syndrome' protein, *Nature 399*, 379−383.
46. Rudolph, M. G., Bayer, P., Abo, A., Kuhlmann, J., Vetter, I. R., and Wittinghofer, A. (1998) The Cdc42/Rac interactive binding region motif of the Wiskott Aldrich syndrome protein (WASP) is necessary but not sufficient for tight binding to Cdc42 and structure formation, *J. Biol. Chem. 273*, 18067−18076.

BI701539X